P.-A. Schnegg, University of Neuchâtel

# A scheme for 3D MT modelling using polynomials

## Introduction

The 3D MT modelling scheme described here employs a forward calculation developed at the Earth Resources Laboratory of the MIT, Cambridge, U.S.A. (Mackie, Madden et al. 1993; Mackie, Smith et al. 1994). This calculation is based upon the integral form of Maxwell's equations where accelerated conjugate gradient relaxation is used to solve for $H_x$, $H_y$ and $H_z$. Occurrence of Mackie's new forward technique and tremendous, presently available increase of PC computing throughput have given rise to publication of numerous studies directed toward three-dimensional lithologies. Examples of such studies can be found in Pous 1995; Livelybrooks 1996; Masero, Fischer et al. 1997; Park 1997.

So far, some MT researchers carry out 3D modellings in very lengthy ways, modifying by hand the parameters of their conductivity models until they are satisfied with the results. To make the search for the best model a smoother, unattended work, we have incorporated Mackie's code into a main computer programme which automatically handles tedious operations like model build-up, misfit calculation and parameter fitting. At each iteration, the main programme carries out a Mackie's forward calculation. Because every five EM field components are computed in the forward code, it is possible to look for conductivity models which either use a subset of the MT parameters (TE, TM mode and/or vertical magnetic field), or all of the available data in the calculation of the objective function.

There is an important restriction in the search for the best model: Somehow, the conductivity distribution should be described by a limited number of parameters. Moreover, this number must be kept within reasonably small values ($< 20$) to avoid convergence problems caused by over-determination.

## Method description

The scheme implied in the proposed method differs little from the approach used in previous papers on 2D MT modelling (Schnegg 1993; Schnegg 1996),

where the geometry and resistivity of a conducting structure was represented by a set of simple polynomials. Similarly, a conductivity model is described by a set of $k$ given functions

$$F_k(\xi, \psi, p_i), i = 1, n_k$$

of the generalized coordinates $\xi$ and $\psi$ , in which the $n_k$ parameters $p_i$ are controlled by an optimization routine. Depending on the topology of the assumed model, these functions can vary from simple polynomials of the cartesian coordinates $x$ and $y$ (distorted dipping layered structure), to any combination of orthogonal polynomials, like spherical harmonics and Legendre polynomials (required for axi-symmetric geometries found in salt domes, volcanoes with magma chambers, astroblems). Obviously, once a set of functions has been chosen, the model will only assume a limited freedom in its variations of the topology.

The programme flowchart is shown on Fig. 1. The first step is executed only once: Initial values of the parameters and weights are read in. At this stage, preliminary information on the model gained by other methods (1D, 2D magnetotellurics, seismic lines, gravimetry) can be advantageously used. Weights allow for individual adjustment of parameter sensitivities, and can be set to zero to freeze the variation of a given parameter, applying thus deliberate constraints to the model.

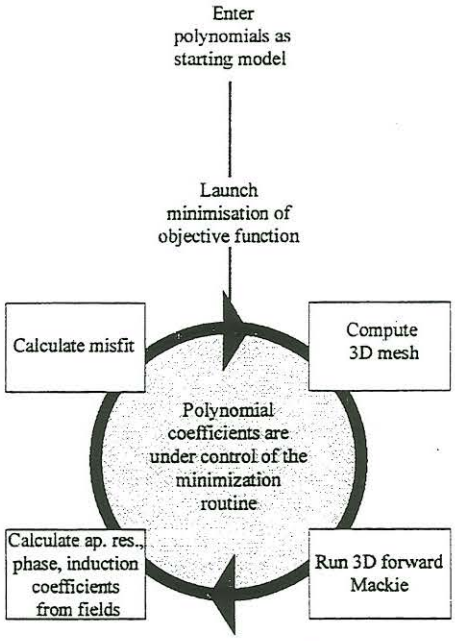

Figure 1: Programme flowchart

The next programme steps are repeated at will in an endless loop or as long as a misfit criterion is not met and occur under control of the optimizing routine. As usually, the misfit is the error between the measured data and the model response, summed over all measuring sites, periods, and polarizations, including apparent resistivities, induction coefficients and their respective phases.

The conductivity model is built up by the programme, according to Mackie's recommendations for mesh design. The resistivity value of the cell located at

coordinates $(x,y)$ is determined by a selected set of functions $F_k$, while the parameters are furnished by the optimizing routine. Forward calculation of the model response is then launched. This is of course the most demanding part of the code, in terms of computing time. Once available, model response is compared to the measured data to yield a misfit value which, in turn, is used by the optimizing routine to alter the parameter set, and determine the steepest descent toward convergence in the parameter space. The computation can run unattended during several hours or days.

## Field example

To illustrate the method on real MT field data, we use the results of a survey carried out in the Penninic Alps of Valais, Switzerland. MT and vertical magnetic field data have been recorded at 24 sites scattered over an area of 60 x 40 km. The Rhone valley represents a natural separation between the external, "helvetic" and internal "penninic" zone of the Central Alps. The helvetic domain corresponds to the south-eastern edge of the former European continent. The penninic zone, on the other hand, consists in a complex stack of basement and cover nappes. Of particular interest to our study is the deepest, northernmost « Zone Houillère ». Its high carbon content, makes this « nappe » a good candidate for a geoelectric anomaly. Moreover, this lithology crops out at the surface along the Rhone river. Laboratory study of drill cores from a nearby borehole evidenced the presence of low-grade carbonated material. Measurements on the samples revealed resistivities as low as 0.6 Ωm. Conductivity increase with hydrostatic pressure indicated reconnection of carbon film at the grain boundaries.

A preliminary 2D modelling was carried out with a subset of sites selected in the neighbourhood of a well-centred profile line. This modelling revealed the shape and extension of a high-conducting, dipping slab, embedded in a resistive rock matrix (Fig.2). We used this model as starting point for the 3D modelling and worked with the full set of MT sites. The region of study was subdivided into 24x14x20 rectangular boxes of size 3x3x0.5 km. Three

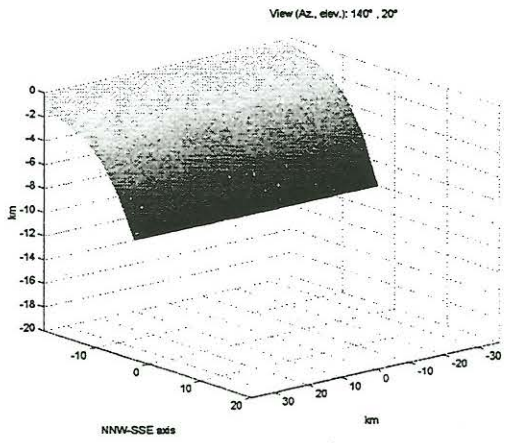


Figure 2: Starting model

columns and three rows were appended on each external side of the model, with increasing widths of 6, 12 and 24 km, dividing thus the space into 30x20x20 blocks. Each vertical slice of this model was embedded in a larger 2D model which extended the regional features. A 1D structure (a half-space in this case) was added at the bottom. This mesh geometry was kept unaltered during the whole modelling process. Only the cell resistivities were allowed to vary.

According to the results of the 2D modelling, we restricted the 3D topology to models which could also be described by 3 layers only. The slab resistivity and thickness were given fixed values of 0.2 Ωm and 1 km. The parameters which have been automatically fitted by the programme are the decimal logarithms of

- the slab depth, $f_1(x,y)$,
- the resistivity of the rock matrix above the slab, $f_2(x,y)$,
- the resistivity of the rock matrix beneath the slab, $f_3(x,y)$.

(Note that we used logarithms instead of the value itself to avoid zero crossing of the resistivity and thickness). These parameters are polynomials of the coordinates $x$ and $y$ with degrees set (quite arbitrarily, but with regard to computing resources) to 3, 2 and 2 respectively. No vertical resistivity variation was allowed within a given layer. Constant polynomials have been given to initialize $f_2$ and $f_3$.

Because computing time is proportional to the number of period values at which the misfit is calculated, we restricted the values to 1 and 100 seconds. 3D view of the final model after 400 iterations is shown in Fig. 3.

The result of the 3D modelling must be regarded as semi-quantitative only, since many simplifications were required to ease the computing task (constant thickness and resistivity of the slab). However the model clearly shows that the shape of the conducting slab strongly departs from a cylindrical geometry and closely matches the uppermost crustal boundary, as determined with seismic profiles (Valasek 1997). There is no doubt that the real shape of the conducting body is more complicated than can be described by our 3D model. However,

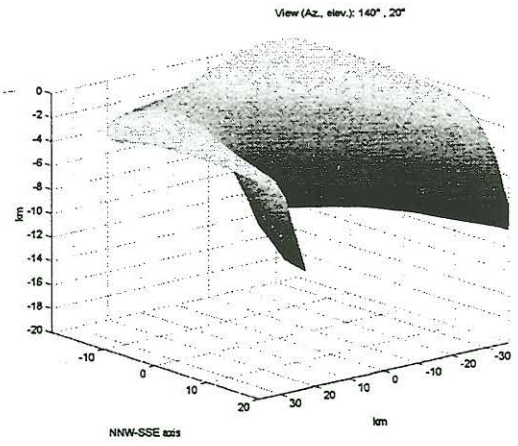


Figure 3: 3D view of the final model

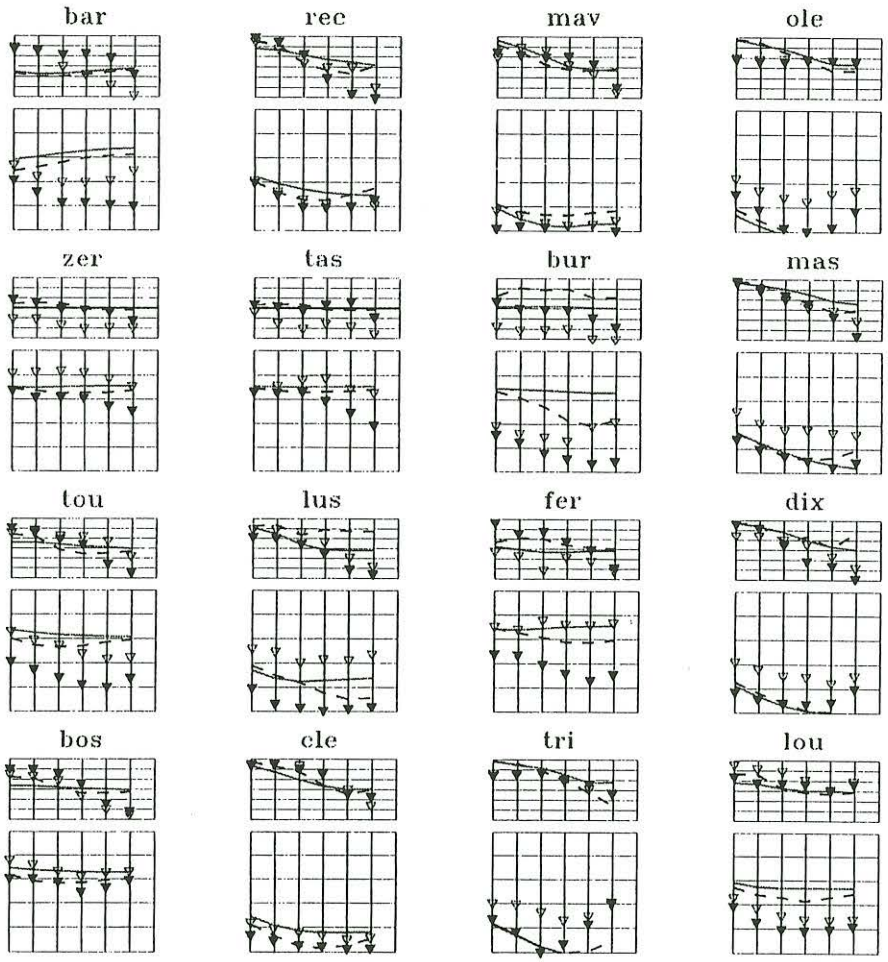


Figure 4: Comparison of measured MT apparent resistivity and phase (triangles) with final model response (lines). Logarithms of resistivities vary between 0 and 5. Phase varies between 0 and 90°. Filled symbols and dashed lines denote the mode in which electric current flows parallelly to Rhone valley.

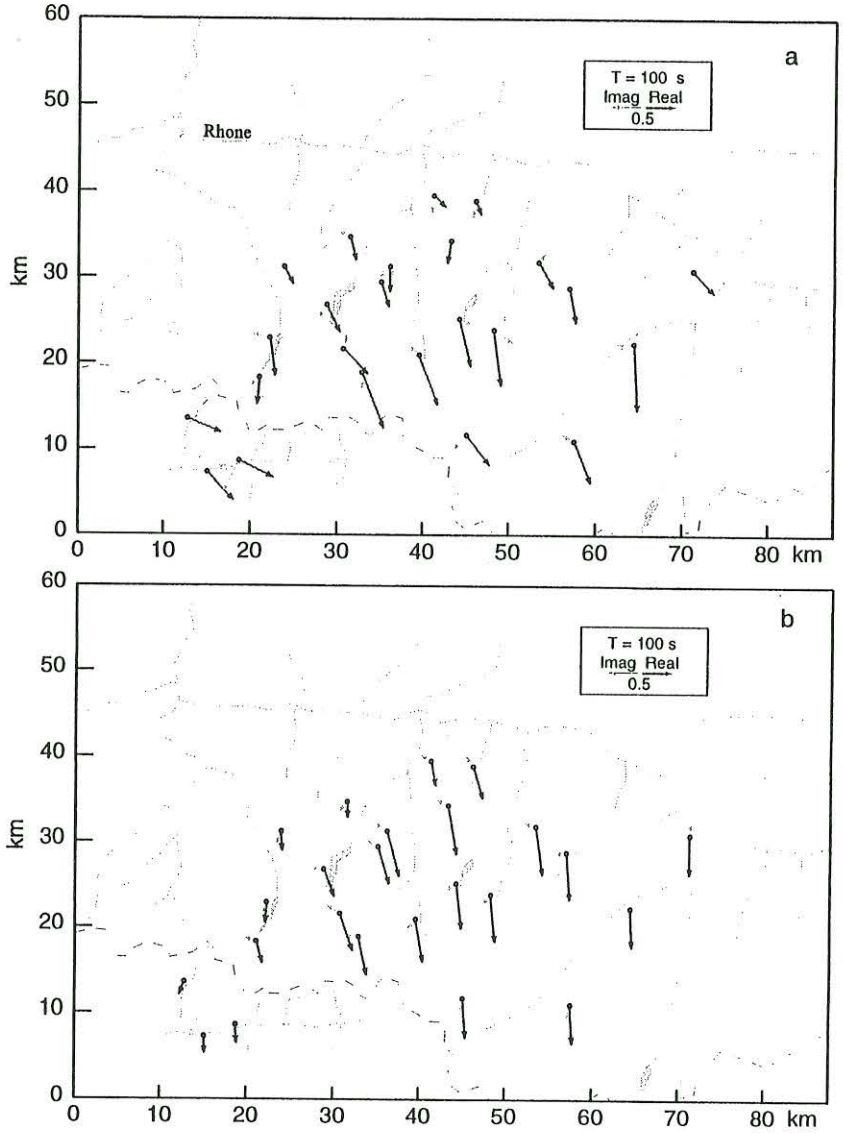


Figure 5: Real and imaginary induction arrows for (a) measured data and (b) response of model shown in Fig. 3 .

the general trend should not differ significantly from the reality, since it displays the same curvature as the Alpine arc and shows a marked depression matching the large scale geometry of tectonic units bordered by features such as the external crystalline massif domes and the Rawil saddle to the NW and the Insubric backfold to the south-east.

The final model response is compared with the field data on Fig. 4 (MT) and Fig. 5 (induction arrows). The misfit of the model response is noticeably larger for 3D than for 2D modelling. The cause is obviously the oversimplification of the 3D model and the limited number of period values which were imposed by the computing time requirements. Moreover, static effects are likely to occur on MT data recorded on such rough topographic area. However, the quite large number of sites used in the modelling mitigates somehow these effects. Because real induction data was significantly better than MT, in terms of scatter, we gave them a weight of 3, compared to 1 for MT.

We also noticed that the modelling scheme was able to converge almost as fast if a non-dipping conducting slab was given as starting model.

## Conclusion

Modelling 2D and 3D MT data by hand can be a very wearing task. Quite frequently, automated methods like the one presented here, can be used successfully, feeding the computer programme with a good guessed initial model, and leaving the modelling work unattended during several days.

Every smooth geologies without lateral discontinuities of the resistivity can be approximated by simple polynomial expressions. This is particularly the case for structures produced in collisions (or extensions; suture zones, crustal décollements and shear zones). Discontinuities can be dealt with by combining several polynomials, or by adding appropriate boundary conditions, at the expense of enhanced computing task, however. The only (but important) point requiring some feeling lies in the correct choice of parameters.

## References


Livelybrooks, D., Mareschal, M., Blais, E., Smith, J.T. (1996). "Magnetotelluric delineation of the Trillabelle massive sulfide body in Sudbury, Ontario." Geophysics **61**(4): 971-86.

Mackie, R. L., T. R. Madden, et al. (1993). "Three-dimensional magnetotelluric modeling using difference equations - theory and comparison to integral equation solutions." Geophysics **58**: 215-226.

Mackie, R. L., J. T. Smith, et al. (1994). "Three-dimensional electromagnetic modeling using finite difference equations: the magnetotelluric example." Radio Science: 923-935.

Masero, W., G. Fischer, et al. (1997). "Crustal deformation in the region of the Araguainha impact, Brazil." Phys. Earth Planet. Inter. **101**: 271-289.

Park, S. K., Mackie, R.J. (1997). "Crustal structure at Nanga Parbat, northern Pakistan, from magnetotelluric soundings." Geophys. Res. Lett. (USA) **24**(19): 2415-18.

Pous, J., Ayala, C., Ledo, J., Marcuello, A., Sabat, F. (1995). "3D modelling of magnetotelluric and gravity data of Mallorca island (Western Mediterranean)." Geophys. Res. Lett. (USA) **22**(6): 735-738.

Schnegg, P.-A. (1993). "An Automatic Scheme for 2-D Magnetotelluric Modelling, Based on Low-Order Polynomial Fitting." J. Geomag. Geoelectr. **45**(9): 1039-1043.

Schnegg, P.-A. (1996). Comparison of 2D modelling methods: rapid inversion vs polynomial fitting. Elektromagnetische Tiefenforschung, Burg Ludwigstein, Deutsche Geophysikalische Gesellschaft.

Valasek, P., Mueller, St. (1997). A 3D crustal model of the Swiss Alps based on an integrated interpretation of seismic refraction and NRP 20 seismic reflection data. Deep structure of the Swiss Alps, Birkhäuser Verlag.